Multi-constrained Motion Planning of a Planar Type Humanoid Using Kinematic Redundancy

Jae Yeon Choi, Youngjin Choi, and Byung-Ju Yi

School of Electrical Engineering and Computer Science, Hanyang University, Ansan, Korea
(Tel : +82-31-416-6417; E-mail: bj@hanyang.ac.kr)

Abstract: The human being carries out multiple works simutaneously. Generally, two legs are constrained to the ground while two arms are performing some other jobs. Sometimes not only two legs but also any parts of the human body such as hand, elbow, head, etc. are kinematically constrained to the environment for special purpose. Sawing motion is one example of the multi-constrained motions. When a person saws a wood, two legs are constrained to the ground and one arm holds the object being sawn on the table so that another arm carries out a stable sawing task. In this paper, we introduces a new motion planning algorithm for a multi-constrained planar type humanoid robot, which exploits "redundant degrees of freedom" of the whole-body humanoid structure. A sequential redundancy resolution algorithm is employed, which ensures the ZMP stability and the planned multi-constrained motion. The feasibility of the proposed algorithm is verified by simulating a sawing motion for a planar humanoid model.

Keywords: Kinematic redundancy, Multi-constrained motion, Sawing task.

1. INTRODUCTION

The human-body has inherent kinematic redundancy in its structure. The redundant system has more degrees of freedom than the required degrees of freedom. Kinematic redundant system has several advantages that can generate various motions using self-motion.

There have been many researches on humanoid motion planning and control [1-15] and the whole-body coordination and control [16-20]. The motion control and the whole body coordination (control) with good performance have been the core parts in implementing the stable humanoid motion.

Since Vukobratovic proposed the concept of ZMP in 1970 [1], it has been the criterion of the stability of biped robots in dynamic motions. Also, a number of researchers have tried to find how to compensate the ZMP trajectories. Kim, et al. [3] proposed a real-time ZMP compensation method using null motion for a simple mobile manipulator. Li, et al. [4] proposed a learning control as a ZMP compensation algorithm for a biped robot having a trunk. Dasgupta, et al. [5] made feasible walking motion based on ZMP with HMCD (Human Motion Capture Data). Park, et al. [6] proposed an off-line method to design a ZMP trajectory with a fuzzy logic. Kurazume [7] proposed a sway compensation trajectory for a biped robot to design a stable ZMP trajectory easily. Sugihara and Nakamura [8] utilized an inverted pendulum method for stable walking. Chevallereau, et al [9] employed the concept of virtual constraints to achieve different tasks for a biped robot RABIIT. Westervelt, et al [10] proved the stability of walking control for planar biped robot. Choi, et al [15] suggested the kinematic resolution method of CoM (center of mass) Jacobian at the level of joint velocity in order to control the ZMP. Sentis, et al [16] proposed the synthesis method of whole body behaviors. Goswami, et al [17] utilized the rate of change of angular momentum as the criterion of balancing motion.

Harada, et al [18-19] proposed the available measure for the whole body coordination of humanoid robot.

Contact is inevitable in human daily life. The contact is regarded as happening of kinematic constraint. In this paper, we introduce a motion planning algorithm for redundant planar type humanoid robot in multi-constrained conditions. The motion of a multi-constrained body varies dynamically according to a partial change of the robot topology. And, depending upon what part of the human body contacts the environment decides the constraint condition. Also, the operation efficiency differs according to the constraint condition. For example, a straddled leg posture is more stable than non-straddled leg posture.

This work initially explains the concept of multi-constrained motion via a sawing task and redundancy resolution algorithms exploiting the kinematic redundancy of the humanoid structure are introduced to realize the task of multi-constrained motion.

## 2. CONCEPT OF MULTI-CONSTRAINED MOTION

2.1 A sawing motion planning algorithm

Consider a planar redundant humanoid model given by Fig. 1. The lower-extremities of two postures are modeled as 3DOF structure. Fig. 1(a) is a single support case and Fig.1(b) is a double support case, and the upper-extremities are modeled as 3DOF serial structure. The lower-extremity is constrained to the ground, and one arm is holding the object on the table and another arm carries out the sawing task.

This kind of situation can be interpreted as a multi-constrained motion because one upper-extremity and two lower-extremities are fixed to the environment, while another arm is performing a sawing task. When the operating arm changes its configurations, the center

of gravity of the humanoid structure is changed. Thus the stability of posture can not be assured. For example, the ZMP (Zero Moment Point) may get out of the foot print. To resolve this problem, a new motion planning algorithm should be developed. This algorithm should be able to assure the ZMP stability, maintain the position of the constrained arm, while successfully performing the desired sawing task. In order to implement this algorithm, a sequential redundancy resolution algorithm will be employed, which exploits the kinematic redundancy inherent in the humanoid structure.

Furthermore, the optimal posture needs to be investigated. If the speed of the sawing motion increases, the ZMP stability cannot be assured because the position of ZMP may get out of the foot print. This case happens when the lower-extrimity maintains the posture shown in Fig. 1(a). On the other hand, when the lower-extrimity has a straddled posture like Fig. 1(b), there is a small chance that ZMP gets out of the foot print even though the speed of the sawing motion increases. Thus the optimal posture of a humanoid structure should be decided with consideration of specifications of the given task.
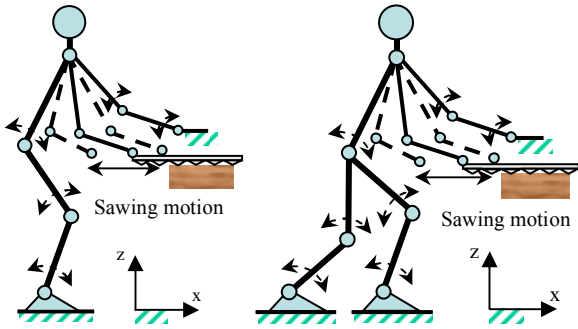
(a) Non-straddled leg posture   (b) Straddled leg posture
Fig. 1. Sawing motion of a planar type humanoid model

3. MOTION PLANNING ALGORITHM USING ZMP CONSTRAINT EQUATION

The ZMP constraint equation can be directly derived by inserting the kinematic relation of each acceleration component into the ZMP equations given by

$$x_{ZMP} = \frac{\sum_i m_i(\ddot{z}_i - g)x_i - \sum_i m_i\ddot{x}_i z_i - \sum_i (\tau_i)_y - \sum_k r_{zk}F_{xk}}{\sum_i m_i(\ddot{z}_i - g)} , \quad (1)$$

$$y_{ZMP} = \frac{\sum_i m_i(\ddot{z}_i - g)y_i - \sum_i m_i\ddot{y}_i z_i + \sum_i (\tau_i)_x}{\sum_i m_i(\ddot{z}_i - g)} , \quad (2)$$

where all the kinematic variables are referenced to the foot coordinate system attached to the center of the support foot. And, each $\ddot{x}_i$, $\ddot{y}_i$, $\ddot{z}_i$, τ_i, m_i and g denotes accelerations, inertia moment, mass of the *i-th* link, and gravitational constant. F_{zk} and r_{xk} denote the *k-th* reaction force by sawing task and the *k-th* position vector referenced to the origin coordinate.

Eq. (1) and Eq. (2) can be rewritten as follows:

$$\sum_i m_i(\ddot{z}_i - g)x_{ZMP} = \sum_i m_i(\ddot{z}_i - g)x_i - \sum_i m_i\ddot{x}_i z_i - \sum_i (\tau_i)_y \\ - \sum_k r_k F_k \quad (3)$$

and

$$\sum_i m_i(\ddot{z}_i - g)y_{ZMP} = \sum_i m_i(\ddot{z}_i - g)y_i - \sum_i m_i\ddot{y}_i z_i + \sum_i (\tau_i)_x . \quad (4)$$

Rearranging Eq. (3) and Eq. (4), we can obtain the following equations

$$\sum_i m_i\ddot{z}_i(x_i - x_{ZMP}) - \sum_i m_i\ddot{x}_i z_i - \sum_i (\tau_i)_y = C_x \quad (5)$$

and

$$\sum_i m_i\ddot{z}_i(y_i - y_{ZMP}) - \sum_i m_i\ddot{y}_i z_i + \sum_i (\tau_i)_x = C_y , \quad (6)$$

where

$$C_x = \sum_i m_i g(x_i - x_{ZMP}) + \sum_k r_k F_k \quad (7)$$

and

$$C_y = \sum_i m_i g(y_i - y_{ZMP}) . \quad (8)$$

The inertial moment exerted at the center of the *i-th* link expressed as

$$\underline{\tau}_i = [I_i]\dot{\underline{\omega}}_i + \underline{\omega}_i \times [I_i]\underline{\omega}_i . \quad (9)$$

can be also written as

$$\underline{\tau}_i = [I^{jk}]\dot{\underline{\omega}}_i + \underline{\omega}_i^T [P^{jk}]\underline{\omega}_i , \quad (10)$$

where $\underline{\omega}_i = [G_i^{jk}]\dot{\underline{\theta}}$.

Similarly, the acceleration of the operational space (i.e., the end position of the model of Fig. 1) can be written by

$$\ddot{\underline{u}} = [G]\ddot{\underline{\theta}} + \dot{\underline{\theta}}^T [H]\dot{\underline{\theta}} . \quad (11)$$

Also, the acceleration of the *i-th* center of mass can be expressed as

$$\ddot{\underline{u}}_i = [G_i]\ddot{\underline{\theta}}_i + \dot{\underline{\theta}}_i^T [H_i]\dot{\underline{\theta}}_i \quad (12)$$

which can be decomposed as three components

$$\ddot{x}_i = [G_i]_{1;}\ddot{\underline{\theta}}_i + \dot{\underline{\theta}}_i^T [H_i]_{1;;}\dot{\underline{\theta}}_i ,$$

$$\ddot{y}_i = [G_i]_{2;}\ddot{\underline{\theta}}_i + \dot{\underline{\theta}}_i^T [H_i]_{2;;}\dot{\underline{\theta}}_i ,$$

and

$$\ddot{z}_i = [G_i]_{3;}\ddot{\underline{\theta}}_i + \dot{\underline{\theta}}_i^T [H_i]_{3;;}\dot{\underline{\theta}}_i ,$$

where $[G_i]_{j;}$ denotes the *j-th* row of $[G_i]$ and $[H_i]_{j;;}$ denotes the *j-th* plane of three dimensional array $[H_i]$[21].

Substituting the three components and the inertial moment term into Eq. (5) and Eq. (6) yields the so called "ZMP constraint equation" given by

$$\underline{C} = \begin{pmatrix} C_x \\ C_y \end{pmatrix} = [G_m]\ddot{\underline{\theta}} + \dot{\underline{\theta}}^T [H_m]\dot{\underline{\theta}} , \quad (13)$$

where assuming that N is the number of joints, we have

$$[G_m] = \sum_i \begin{bmatrix} m_i(x_i - x_{ZMP})[G_i]_{3;} - m_i z_i[G_i]_{1;} - \{[I_i^{jk}][G_i^{jk}]\}_{2;} \\ m_i(y_i - y_{ZMP})[G_i]_{3;} - m_i z_i[G_i]_{2;} + \{[I_i^{jk}][G_i^{jk}]\}_{1;} \end{bmatrix} \in \Re^{2 \times N}$$

and the matrices consisting of $[H_m]$ are

$$[H_m]_{1;;} = \sum_i \Big[m_i(x_i - x_{ZMP})[H_i]_{3;;} - m_i z_i[H_i]_{1;;} - \{[I_i^{jk}] \circ [G_i^{jk}] + [G_i^{jk}]^T [P_i^{jk}][G_i^{jk}]\}_{2;} \Big] \in \Re^{2 \times N}$$

$$[H_m]_{2;;} = \sum_i \left[m_i(y_i - y_{ZMP})[H_i]_{3;;} - m_i z_i [H_i]_{2;;} + \left\{ [I_i^{jk}] \circ [G_i^{jk}] + [G_i^{jk}]^T [P_i^{jk}][G_i^{jk}] \right\}_{1;;} \right] \in \Re^{2 \times N}.$$

Eq. (13) is the ZMP constraint equation, where $\underline{C}$, $[G_m]$, and $[H_m]$ are known, which are function of the dynamic parameters of the planar type humanoid robot system.

When the system has enough kinematic redundancy, the general solution of the ZMP constraint equation (13) is described as

$$\ddot{\underline{\theta}} = [G_m]^+ (\underline{C} - \dot{\underline{\theta}}^T [H_m]\dot{\underline{\theta}}) + (I - [G_m]^+[G_m])\underline{\varepsilon}, \qquad (14)$$

where '+' denotes the pseudo-inverse operator and $\underline{\varepsilon}$ is an arbitrary vector.

The first term of Eq. (14) denotes the minimum norm solution. Similar to kinematically redundant manipulators, the inertia weigthed pseudo-inverse solution of $[G_m]$ yields a dynamically-consistent motion as proposed by Khatib [22].

The second term of Eq. (14) denotes the homogeneous solution, which can be used for controlling the desired operational trajectory such as the sawing motion of the hand.

Now, for the given desired operational trajectory $\underline{u}(t)$, substituting Eq. (14) into Eq. (11) results in the solution of $\underline{\varepsilon}$ given by

$$\underline{\varepsilon} = [G(I - [G_m]^+[G_m])]^+(\ddot{\underline{u}} - G[G_m]^+(\underline{C} - \dot{\underline{\theta}}^T[H_m]\dot{\underline{\theta}}) - \dot{\underline{\theta}}^T[H]\dot{\underline{\theta}}) . (15)$$

It is to note that the solution of Eq. (14) sequentially guarantees the desired ZMP trajectory and the desired operational trajectory. The joint angles can be obtained by numerically integrating the angular acceleration vector twice with respect to time.

4. SIMULATION STUDIES

In order to verify the proposed motion planning algorithm, we perform simulation for a sawing task which has multi-constrained motion. In the sawing task, it is necessary to increase the external impulse applied to the object being sawn. Thus, optimal posture of the sawing task, which generates best performance in external impulse, should be investigated.

5.1 External impulse model for a sawing task

In order to obtain the dynamic model of general hybrid mechanism containing serial-chains as well as closed-chains, we convert the system as an open-tree structure as shown in Fig. 2. The open-tree structure is made by cutting joints of closed-chains. From the open-tree structure, the dynamic model of each serial-chain is evaluated. Then, the dynamic model for the open-tree structure referenced to the Laragian coordinate set ϕ is represented as

$$\underline{T}_\phi = [I_{\phi\phi}^*]\ddot{\underline{\phi}} + \dot{\underline{\phi}}^T[P_{\phi\phi}^*]\dot{\underline{\phi}}, \qquad (16)$$

where $[I_{\phi\phi}^*]$ represents the inertia matrix $[P_{\phi\phi}^*]$ represents the inertia power array, and $\underline{T}_\phi$ is the force or torque vector for joint ϕ.
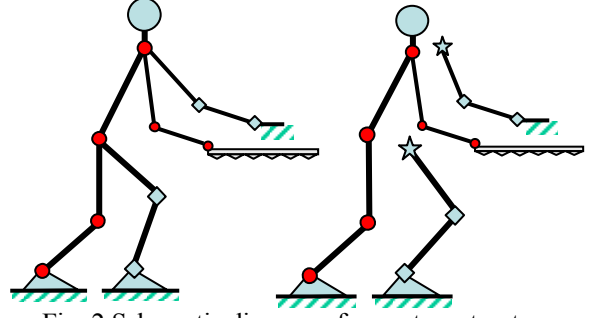

Fig. 2 Schematic diagram of open-tree structure
(○: Independent joint, ☆: Cut joint)

Next, using the principle of virtual work, we incorporate the dynamics of the open-tree structure into a dynamic model in terms of the independent coordinates. It is given by

$$\underline{T}_a = [I_{aa}^*]\ddot{\underline{\phi}}_a + \dot{\underline{\phi}}_a^T[P_{aaa}^*]\dot{\underline{\phi}}_a \qquad (17)$$

where $[I_{aa}^*]$ represents the inertia matrix $[P_{aaa}^*]$ represents the inertia power array, and $\underline{T}_\phi$ is the inertial load vector referenced to the independent joint set [21].

When a robot saw the material, the dynamic model of the robot referenced to the independent joint set is given by

$$\underline{T}_a = [I_{aa}^*]\ddot{\underline{\phi}}_a + \dot{\underline{\phi}}_a^T[P_{aaa}^*]\dot{\underline{\phi}}_a - [G_a^{\upsilon_I}]\underline{F}_{ext} \qquad (18)$$

where $\underline{F}_{ext}$ is the impulsive external force at the contact point and $[G_a^{\upsilon_I}]$ denotes the first order KIC(Kinematic Influence Coefficient) relates the contact point's velocity $\underline{\upsilon}_I$ with respect to the independent joint's velocity.

Integration of the dynamic model given in Eq. (18) over contacting time interval gives

$$\int_{t_0}^{t_0+\Delta t} \underline{T}_a dt = \int_{t_0}^{t_0+\Delta t} [I_{aa}^*]\ddot{\underline{\phi}}_a \, dt + \int_{t_0}^{t_0+\Delta t} \dot{\underline{\phi}}_a^T[P_{aaa}^*]\dot{\underline{\phi}}_a \, dt$$
$$- \int_{t_0}^{t_0+\Delta t} [G_a^{\upsilon_I}]^T \underline{F}_{ext} dt \qquad (19)$$

Since the positions and velocities are assumed finite all the time during impact, the integral term involving $\dot{\underline{\phi}}^T[P_{aaa}^*]\dot{\underline{\phi}}$ becomes zero as Δt goes to zero, as does the term involving actuation input $\underline{T}$. Thus, we obtain the following simple expression

$$[I_{aa}^*]\left(\dot{\underline{\phi}}(t_0 + \Delta t) - \dot{\underline{\phi}}(t_0)\right) = [G_\phi^{\upsilon_I}]^T \underline{\tilde{F}}_{ext}, \qquad (20)$$

where $\underline{\tilde{F}}_{ext} = \int_{t_0}^{t_0+\Delta t} \underline{F}_{ext} dt$ is defined as the external impulse at the contact point. Thus, the velocity increment of the joint variables is

$$\Delta\dot{\underline{\phi}}_a = [I_{aa}^*]^{-1}[G_a^{\upsilon_I}]^T \underline{\tilde{F}}_{ext} \qquad (21)$$

and the velocity increment at the contact point is obtained by the following kinematic relationship.

$$\Delta\underline{\upsilon}_I = [G_a^{\upsilon_I}]\Delta\dot{\underline{\phi}}_a = [G_a^{\upsilon_I}][I_{aa}^*]^{-1}[G_a^{\upsilon_I}]^T \underline{\tilde{F}}_{ext} \qquad (22)$$

Assuming that the sawn chip is very small, deforms permanently (i.e, $e = 0$) and the object to be sawn is initially stationary, the velocity increment of sawing

chip is negligible.

Finally, the external impulse can be evaluated as follows:

$$\tilde{F}_{ext} = \frac{-(\underline{v}_I)^T \underline{n}}{\underline{n}^T \{ [\boldsymbol{G}_{aa}^{v_I}][\boldsymbol{I}_{aa}^*]^{-1}[\boldsymbol{G}_a^{v_I}]^T \} \underline{n}} \, , \qquad (23)$$

where $\underline{n}$ denotes a vector normal to the contact surface.

Now, the external force exerted on the object being sawn is obtained, in real time, by the product of the external impulse and the sampling time.

5.2 Sawing motion of a planar Humanoid robot using motion planning algorithm

Fig. 3(a) and Fig. 4(a) show one cycle sawing motion for the non-straddled and the straddled leg posture, respectively. According to Eq. (14), the planar type humanoid successfully maintains its initial ZMP stably while performing the forth and back sawing motion as shown in Fig. 3(b) and Fig. 4(b).

Also, the external impulse changes according to the configuration of the planar type humanoid. Fig. 5 depicts the external impulse with respect to the time. We would like to analyze the external impulse with respect to the posture, speed, and so on.
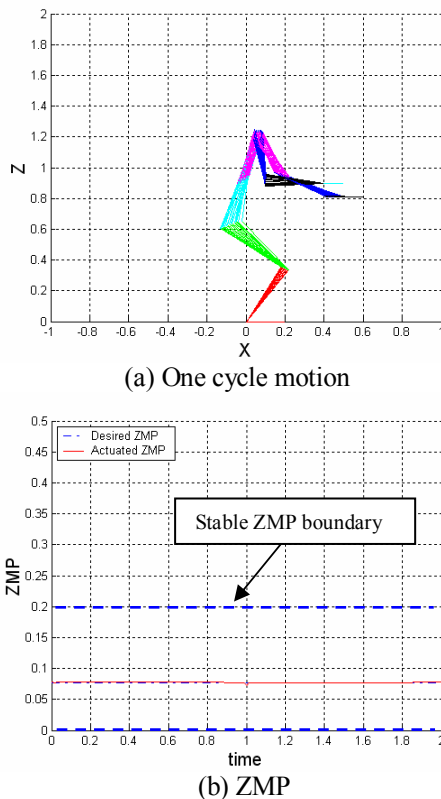

(a) One cycle motion

(b) ZMP

Fig. 3. Sawing motion of the non-straddled leg posture
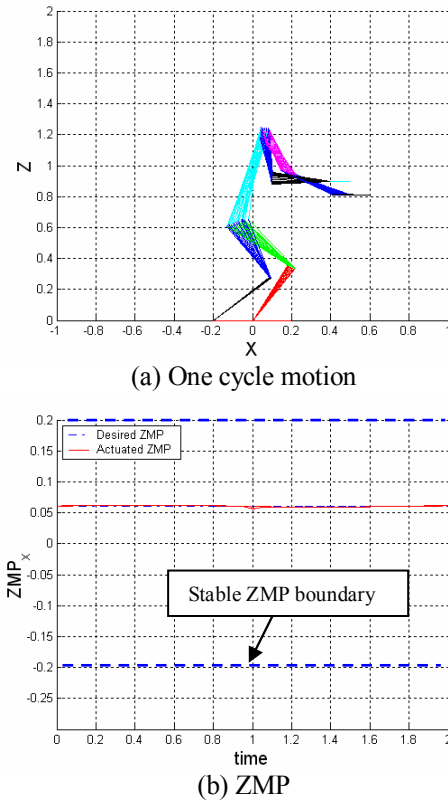

(a) One cycle motion

(b) ZMP

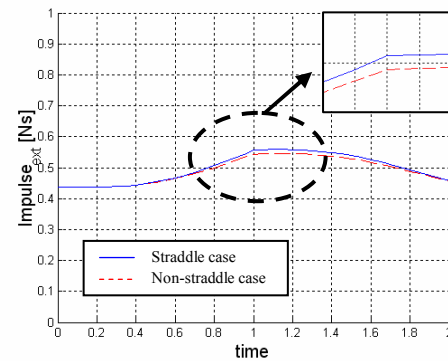Fig. 4. Sawing motion of the straddled leg posture

Fig. 5. External impulse

5.3 Comparison of the non-straddled leg posture with the straddled leg posture for the sawing motion

To look for the optimal condition of the sawing task, we consider three cases as shown in Table 1. In the case 1, we increase the sawing velocity. In the case 2, we design a variable ZMP trajectory as shown in Fig. 6. It is remarked that the stable ZMP boundary region at the straddled leg posture is much larger than that of the non-straddled leg posture. The case 3 combines the cases 1 and 2. Fig. 7 shows that the external impulse becomes larger when the arm is stretched out (in the middle part of the plot) and that it is proportional to the speed and that the straddled leg posture yields more external impulse.

625

Table 1. Three cases

Case 1	Increase the sawing velocity twice
Case 2	Input the ZMP trajectory
Case 3	Combine the case 1 and 2
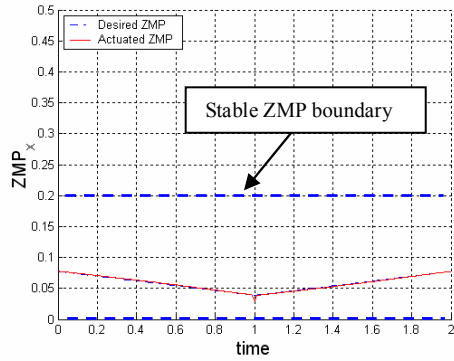
(a) Non-straddled leg case
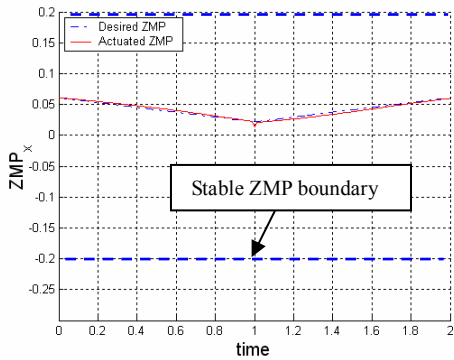
(b) Straddle leg case

Fig. 6. ZMP trajectory

Conclusively, the straddled leg posture is advantageous on the sawing task because it assures larger ZMP stable region as compared to the non-straddled leg posture.

6. CONCLUSIONS

The major contribution of this paper is to propose a motion planning algorithm in multi-constrained robot tasks. A sequential redundancy resolution algorithm is proposed, which ensures the ZMP stability and the planned multi-constrained sawing motion. The feasibility of the proposed algorithm was verified by simulation.
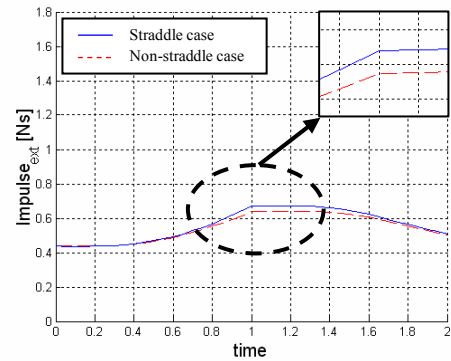
As the future work, the proposed motion planning algorithm can be possibly extended to the general type of multi-constrained motion of the humanoid. And its experimental verification is an ongoing subject.
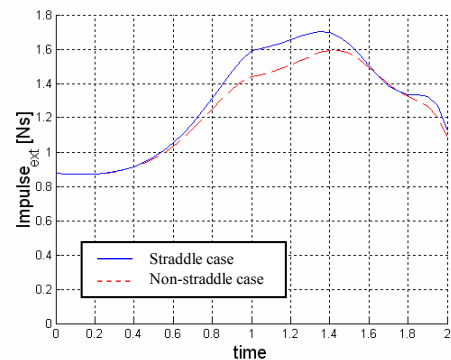
ACKNOWLEDGEMENT
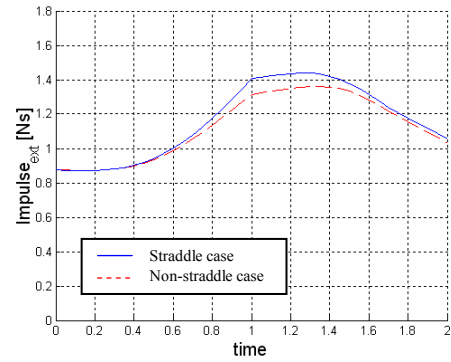
(a) Case 1

(b) Case 2

(c) Case 3

Fig. 7. External impulse of the each case

REFERENCES

[1] M. Vukobratovic, A.A. Frank, and D. Jricic, "On the stability of biped locomotion," *IEEE Trans. on Biomedical Engineering*, BME17-1, pp. 25-36, 1970.

[2] F. Amironche, C. Tung, G. Andersson, and R. Natarajan, "Redundancy modeling of optimum lifting conditions," in *Advances in Bioengineering Proc. of ASME Design Conf.*, BED-Vol. 20, pp. 509-512, 1991.

[3] J. Kim, W. Chung, Y. Youm, and B. Lee, "Real-time ZMP compensation method using null motion for mobile manipulators," in *Proc. of IEEE Int. Conf. on Robotics and Automation*, pp. 1967-1972, 2002.

[4] Q. Li, A. Takanishi and I. Kato, "Learning control for a biped robot with a trunk," in *Proc. of IEEE/RSJ Int. Conf. on Intelligent Robots and*

systems, pp. 1771-1777, 1993.

[5] A. Dasgupta and Y. Nakamura, "Walking feasible walking motion of humanoid robotics from human motion capture data," in *Proc. of IEEE Int. Conf. on Robotics and Automation*, pp. 1044-1049, 1999.

[6] J.H. Park and Y.K. Rhee, "ZMP trajectory generation for reduced trunk motions of biped robots," in *Proc. of IEEE Int. Conf. on Intelligent Robots and Systems*, pp. 90-95, 1998.

[7] R. Kurazume, T. Hasegawa, and K. Yoneda, "The sway compensation trajectory for a biped robot," in *Proc. of IEEE Int. Conf. on Intelligent Robots and Systems*, pp. 925-931, 2003.

[8] T. Sugihara and Y. Nakamura, "Contact phase invariant control for humanoid robot based on variable impedant inverted pendulum model," *IEEE Transactions on Robotics and Automation*, pp. 51-56, 2003.

[9] C. Chevallereau, G. Abba, Y. Aoustin, F. Plestan, E.R. Westervelt, C. Canudas-de-Wit, and J.W. Grizzle, "RABBIT: A testbed for advanced control theory," *IEEE Control Systems Magazine*, vol. 23, no. 5, pp. 57-79, October, 2003.

[10] E.R. Westervelt, J. W. Grizzle, and D. E. Koditschek, "Hybrid Zero Dynamics of Planar Biped Walkers," *IEEE Trans. on Automatic Control*, vol. 48, no. 1, pp. 42-56, 2003.

[11] A. Takanishi, H. Lim, M. Tsuda, and I. Kato, "Realization of Dynamic Biped Walking Stabilized by Trunk Motion on a Sagitally Uneven Surface," in *Proc. of IEEE/RSJ Int. Conf. on Intellgent Robots and Systems*, pp. 323-330, 1990.

[12] Q. Huang, S. Sugano, and I. Kato, "Stability control for a mobile manipulator using a potential method," in *Proc. of IEEE/RSJ Int. Conf. on Intelligent Robots and Systems,* pp. 832-838, 1993.

[13] Q. Huang, K. Yokoi, S. Kajita, K. Kaneko, H. Arai, N. Koyachi, and K.Tanie, "Planning walking patterns for a biped robot," *IEEE Transactions on Robotics and Automation*, vol. 17, no. 3, pp. 280-289, 2001.

[14] D. Yoo, B. So, J. Choi, and B.-J. Yi, "Study on redundancy resolution algorithm of humanoid," in *Proc. of Int. Conf. on Control, Automation and Systems*, pp. 2759-2764, 2003.

[15] Y. Choi, D.Kim, and B.J. You, "On the Walking Control for Humanoid Robot based on the Kinematic Resolution of CoM Jacobian with Embedded Motion," in *Proc. of IEEE/RSJ Int. Conf. on Intellgent Robots and Systems*, pp. 2655-2660, May, 2006.

[16] L. Sentis and O. Khatib, "Synthesis of whole-body behaviors through hierarchical control of behavioral primitives," *International Journal of Humanoid Robotics*, vol. 2, no.4, pp. 505-518, Dec., 2005.

[17] A. Goswami and V. Kallem, "Rate of chage of angular momentum and balance maintenance of biped robots," in *Proc. of IEEE Int. Conf. on Robotics and Automation*, pp. 3785-3790, 2004.

[18] K. Harada, S. Kajita, K. Kaneko, and H. Hirukawa, "ZMP Analysis for arm/leg coordination," in *Proc. of IEEE Int. Conf. on Robotics and Automation*, pp. 75-81, 2003.

[19] S. Kajita, F. Kanehiro, K. Kaneko, K. Fujiwara, K. Harada, K. Yokoi, and H. Hirukawa, "Resolved momentum control : Humanoid motion planning based on the linear and angular momentum," in *Proc. of IEEE Int. Conf. on Robotics and Automation*, pp. 1644-1650, 2003.

[20] T. Sugihara and Y. Nakamura, "Whole-body coorperative balancing of humanoid robot using COG jacobians," in *Proc. of IEEE/RSJ Int. Conf. on Intellgent Robots and Systems*, pp. 2575-2580, 2002.

[21] R.A. Freeman and D. Tesar, "Dynamic modeling of serial and parallel mechanisms/robotic systems, part I-methodology, part II-application," in *Proc. of 20th ASME Mechanism Conf.*, Orlando, 1988.

[22] Khatib, O., "A unified approach to motion and force control of robot manipulators: The operational space approach," *IEEE Transaction on Robotics and Automation*, vol. 3, no. 1, pp. 43-53, Feb., 1987.

[23] D. Chaffin and G. Andersson, *Occupational biomechanics*, pp. 62-69, 1984.